*Journal of Alloys and Compounds, 194* (1993) 77–85
*JALCOM 532*



# EXAFS study of chemical short-range order in amorphous $Ni_xTi_{1-x}$ alloys

P. Chartier, J. Mimault, T. Girardeau and M. Jaouen
*Laboratoire de Métallurgie Physique, URA 131 CNRS, 40, avenue du Recteur Pineau, 86022 Poitiers Cedex (France)*

G. Tourillon
*Laboratoire d'Utilisation du Rayonnement Electromagnétique, Bâtiment 209 D, 91405 Orsay Cedex (France)*

(Received July 21, 1992; in final form September 23, 1992)

**Abstract**

Extended X-ray absorption fine structure (EXAFS) measurements of amorphous $Ni_xTi_{1-x}$ alloys produced by planar magnetron sputtering were obtained using the transmission detection technique at both Ti and Ni absorption K edges. The local environment was determined around the two atomic species by fitting the filtered EXAFS functions. The result reflects the presence of chemical short-range order (CSRO) which favours unlike atomic bonds. Using Miedema's semi-empirical model, the CSRO in amorphous $Ni_xTi_{1-x}$ is found to be intermediate between that of a random alloy and that of an ordered crystalline alloy. The results are compared with those of other amorphous alloy systems.

## 1. Introduction

Amorphous alloys are of important technological interest due to their specific properties (high corrosion resistance, excellent friction coefficient and high wear resistance) which depend on the mode of preparation. Amorphous NiTi alloys can be obtained in a variety of ways.

(1) By liquid quenching, which produces amorphous alloys in the composition range 25–40 at.% Ni [1]. The microscopic structure of these amorphous materials has been studied using X-ray or neutron diffraction [2–4] and chemical short-range order (CSRO) has been demonstrated by diffraction data, firstly by a small pre-peak in the scattering pattern and secondly by a decrease in the average interatomic distances. The CSRO parameter indicates a preference for unlike neighbours in the alloy. Moreover, Buschow [5] has investigated the influence of the CSRO on the crystallization temperature of amorphous alloys.

(2) By vapour quenching which produces amorphous alloys in the composition range 25–75 at.% Ni [6, 7]. X-Ray diffraction [8] and electron diffraction [9] results reveal the existence of partial CSRO responsible for the formation of a non-stoichiometric $Ni_3Ti$ phase at the beginning of crystallization.

(3) More recently, $Ni_xTi_{1-x}$ alloys have been synthesized by mechanical alloying [10]. Extended X-ray absorption fine structure (EXAFS) data have been obtained [11] on amorphous $Ni_{50}Ti_{50}$ and reveal the existence of CSRO, *i.e.* a preference for unlike atoms in the first coordination shell of nickel and titanium, indicated by a decrease in the average interatomic distances.

In another study of the amorphous $Ni_xTi_{1-x}$ system, Gazzillo *et al.* [12] analysed the scattering data in terms of a non-additive hard-sphere model. Fixing the interatomic distances, they estimated the partial coordination numbers and then deduced the CSRO parameter. This theoretical model accounts for the presence of a pre-peak in the diffraction pattern.

The existence of CSRO, as strong as in amorphous $Ni_xTi_{1-x}$ alloys, accounts for deviations from the ideal case in the calculation of the amorphous to crystalline transformation enthalpy. The crystallization enthalpies of amorphous alloys can be theoretically calculated using Miedema's semi-empirical model [13], and are comparable with the experimental values only when the presence of CSRO is included in the calculations. For several amorphous systems, Weeber [14] collected experimental crystallization enthalpy values in order to determine the CSRO and found that it was intermediate between those related to ordered and random alloys.

This paper reports EXAFS investigations on amorphous $Ni_xTi_{1-x}$ alloys at both Ti and Ni K edges for four atomic concentrations ($x = 0.68$, 0.56, 0.43 and 0.30

0925-8388/93/$6.00

at.%). EXAFS signals are characteristic of the immediate environment of atomic species and are well suited to provide directly the CSRO parameter. Simulations of the filtered EXAFS function provide the average local atomic environment of Ti and Ni atoms.

Details on the sample preparation, EXAFS measurements and analysis procedure are presented. The determination and transferability of the amplitude and phase parameters used for the EXAFS signal simulation are discussed in the case of amorphous alloys. Experimental results, relevant to the four amorphous alloy compositions, are reported and calculation details concerning one particular alloy ($Ni_{68}Ti_{32}$) are developed for the chosen environment model and for the CSRO determination. Finally our results are compared with the general law established from Miedema's semi-empirical model by Weeber [14] for several other amorphous compounds.

## 2. Experimental details

### 2.1. Sample preparation and EXAFS measurements

The amorphous samples were prepared at the Department of Materials Science and Engineering, Stanford University (USA) by planar magnetron sputtering using two magnetron sources with elemental Ti and Ni targets. This technique is described in ref. 15. Films, 8 $\mu$m thick, were obtained after 3 h of deposition. This thickness is suitable for transmission EXAFS measurements. Structural characterizations were performed on four $Ni_xTi_{1-x}$ samples with $x = 0.68$, 0.56, 0.43 and 0.30 at.%. Specimen compositions were determined using electron microprobe analysis and are given with an error of 2 at.%. Edge height magnitudes of the experimental X-ray absorption cross-sections were consistent with the given alloy compositions.

EXAFS measurements were taken at the Laboratoire d'Utilisation du Rayonnement Electromagnétique (LURE), Orsay, France using the synchrotron radiation from the Dipositif de Collisions dans l'Igloo storage ring, operating with an energy of 1.85 GeV and a current of 230 mA.

The X-ray absorption spectra were collected over 800 eV above the nickel K edge (8333 eV) and titanium K edge (4966 eV). Measurements were performed at liquid nitrogen temperature (78 K) in order to reduce the thermal disorder in the probed material and consequently to increase the magnitude of the spectra. To improve the signal-to-noise ratio, two consecutive scans were performed and the current was collected over 2 s for each data point, the energy step being 2 eV. Monochromatization of the incoming beam was achieved using Si ⟨111⟩ (slightly detuned to avoid harmonic generation) and Si ⟨311⟩ channel cut monochromators for the Ti and Ni K edges respectively.

### 2.2. EXAFS analysis procedure

The X-ray absorption spectra were background subtracted and normalized, using a standard procedure, to extract the oscillation part of the EXAFS spectrum $\chi(k)$ given by

$$\chi(k) = [\mu(k) - \mu_0(k)]/\mu_0(k)$$

where $\mu(k)$ is the atomic absorption coefficient. The gaseous absorption coefficient $\mu_0(k)$ was determined by fitting the background with a polynomial law. The polynomial degree and the weighting factor were identical for all spectra. The photoelectron wavevector is given by $k = [(E - E_0)2m/\hbar^2]^{1/2}$ where $E$ is the photon energy and $E_0$ is the zero kinetic energy of the photoelectron. $E_0$ was taken at the inflexion point of the threshold. Fourier transformation (FT) was performed over the range 40–120 $nm^{-1}$ using nodal points ($\chi(k) = 0$) for the Hamming window function, $k^3$ weighted to emphasize the high energy part of the signal. By inverse Fourier transform, the EXAFS contribution of the single first peak of the FT was isolated. Simulation of the EXAFS function was performed using the widely reported formula [16]

$$k\chi_i(k) = \sum_j [f_j(k, \pi)N_j/r_{ij}^2] \exp(2\sigma_{ij}^2 k^2) \times \exp(-2kr_{ij}/\Gamma) \sin[2kr_{ij} + \phi_{ij}(k)] \quad (1)$$

where $N_j|f_j(k, \pi)|$ is the backscattering amplitude of $N_j$ atoms of type $j$ surrounding the absorbing atom of species $i$, a distance $r_{ij}$ apart; $\sigma_{ij}^2$ is the mean square relative displacement (MSRD) assuming a gaussian distribution; the term $\exp(2\sigma_{ij}^2 k^2)$ is also called the Debye–Waller factor; $\exp(-2kr_{ij}/\Gamma)$ is a mean free path term taking into account the inelastic losses; $\phi_{ij}(k)$ is the total phase shift which comes from the backscattering and the central atom phases. The amplitude $|f_j(k, \pi)|$ and the total phase $\phi_{ij}(k)$ are extracted from experimental standard data as described below.

The best fits of an experimental filtered EXAFS function are first found by minimizing a variance defined by

$$V = \sum_i^n [E_{th}^i(0) - E_{exp}^i(0)]^2/n \quad (2)$$

where $E_{th}^i(0)$ and $E_{exp}^i(0)$ represent the nodal energy values of the theoretical and experimental signals respectively. The variance calculation is based on the least-squares fitting of the nodal point positions. Solutions giving a variance between the minimum variance ($V_m$) and twice this value are considered to be technically acceptable.

Of the above-mentioned solutions, we keep those which give the best amplitude agreement. A home-built program is used which minimizes the deviation

between the experimental and theoretical maximum amplitude values of the EXAFS oscillations inside the 40–120 $nm^{-1}$ $k$ range.

*2.3. Amplitude and phase parameters*

In order to obtain different coordination numbers with sufficient confidence, it is first necessary to obtain and test the backscattering amplitudes for titanium and nickel atoms. Backscattering amplitudes have been calculated by Lee and Beni [17]. Stern *et al.* [18] have observed errors of up to 20% between experimental and theoretical backscattering amplitudes in the lowest energy range of the pure copper EXAFS spectrum. To avoid this, we have used theoretical backscattering amplitudes and have adjusted them in order to obtain an excellent fit of the experimental standard signal using the reported structural parameters. To obtain the best fit of the signal, we must apply the appropriate values for the MSRD factor and for the inelastic losses term ($\exp(-2kr_{ij}^2/\Gamma)$) which minimizes the amplitude correction.

For example, pure nickel has an f.c.c. structure in which each atom is surrounded by 12 nickel atoms at 0.249 nm. Using $\sigma_{NiNi}=0.0085$ nm, $\Gamma=4.5$ eV and the structural parameters given above, we obtained the best fit with the experimental data from which we extracted the backscattering amplitude $|f_{Ni}(k, \pi)|$.

Pure titanium has a hexagonal structure with six first nearest neighbours at 0.291 nm and six next nearest neighbours at 0.295 nm. Using the procedure described above for pure nickel, we obtained the backscattering amplitude $|f_{Ti}(k, \pi)|$ with $\sigma_{TiTi}=0.009$ nm and $\Gamma=4.5$ eV for the two subshells. The value $\Gamma=4.5$ eV is used in all further calculations with these backscattering amplitudes.

The total phase shift is also extracted from experimental standard EXAFS signals. From pure titanium and pure nickel signals we have deduced $\phi_{TiTi}(k)$ and $\phi_{NiNi}(k)$.

According to Laves and Wallbaum [19], $Ni_3Ti$ presents a hexagonal structure in which a titanium atom has 12 nickel atoms in its first neighbouring shell, at a distance of 0.255 nm. From the experimental EXAFS functions measured by the transmission mode at the Ti K edge on this standard material, and using the previous structural parameters, we have determined the total phase shift $\phi_{TiNi}(k)$.

The last phase shift, $\phi_{NiTi}(k)$, is simply deduced from the others using the following relation

$$\phi_{NiTi}(k)=\phi_{NiTi}(k)+\phi_{TiTi}(k)-\phi_{TiNi}(k)$$

Thus the backscattering amplitudes and phases have been extracted from three standard reference spectra. A comparison between our experimental phase shift values and those theoretically calculated by McKale *et al.* [20] indicates a difference between the two sets of absolute values (same slopes). Nevertheless, we observe the same relative variation in the 40–120 $nm^{-1}$ $k$ range.

As a first approach to the study of the $Ni_xTi_{1-x}$ system, and in order to test the experimental phases and amplitudes, we have simulated the filtered EXAFS function measured by the transmission mode at room temperature at the Ti and Ni K edges in the crystalline $NiTi_2$ alloy. As reported by Yurko *et al.* [21], $NiTi_2$ is f.c.c., space group $O_h^7$-*Fd3m* (number 227 in the International Tables for X-Ray Crystallography), with 96 atoms in the unit cell and a lattice parameter $a_0=1.1227$ nm. In Table 1 the distances and coordination numbers of $NiTi_2$ calculated from ref. 21 are given which were used to simulate the EXAFS spectra. The fits are excellent with the indicated MSRD and $\Gamma$ values. This enables us to conclude firstly that the EXAFS formula (eqn. (1)) assuming a gaussian distribution is well adapted if we wish to determine structural parameters in a rather complex system, and secondly that the experimental amplitudes and phases deduced as mentioned above can be confidently transferred to study such a complex material.

The transferability of these amplitudes and phases to the case of amorphous alloys must be discussed. The topological disorder which is always present in amorphous alloys makes the use of the same theoretical EXAFS expression (eqn. (1)) questionable. Indeed, the validity of the gaussian distribution function at the lowest interatomic distances (which are theoretically limited) must be checked. In order to minimize this effect and to provide consistency in our calculations, all reference parameters were deduced from experiments performed at room temperature whereas amorphous signals were recorded at liquid nitrogen temperature. Despite this, the MSRD factors obtained from the amorphous signal simulations are still slightly larger than those related to the reference. Therefore it is necessary to discuss the validity of the simulation per-

TABLE 1. Structural parameters of crystalline $NiTi_2$ alloy extracted from ref. 21 and used for the best EXAFS simulation

| Central atom | $N_{AB}$ | Surrounder | $R_{AB}$ (nm) | $\sigma_{AB}$ (nm) |
|---|---|---|---|---|
| Ni | 3 | Ni | 0.282 | 0.011 |
| | 3 | Ti | 0.248 | 0.009 |
| | 3 | Ti | 0.256 | 0.009 |
| | 3 | Ti | 0.289 | 0.009 |
| Ti | 1.5 | Ni | 0.248 | 0.009 |
| | 1.5 | Ni | 0.256 | 0.009 |
| | 1.5 | Ni | 0.289 | 0.009 |
| | 3 | Ti | 0.291 | 0.007 |
| | 3 | Ti | 0.297 | 0.007 |
| | 3 | Ti | 0.303 | 0.007 |

formed with a gaussian atomic distribution by applying the cumulant development based on the results of Bunker [22]. We briefly discuss below how the variance test remains valid if a gaussian pair distribution is used in a limited energy range. The small shift in the interatomic distances and the small change in the coordination numbers obtained from the simulation do not significantly modify the atomic pair ratio or the local chemical order.

## 3. Results

### *3.1. Qualitative approach*

The EXAFS signal of any unknown material results from the total interference process occurring around each absorbing atom. For an amorphous material, the nearest neighbour is different from one atomic site to another. Information contained in the EXAFS signal is provided by all existing configurations, but it may be interpreted as the signal of the most reproducible local picture. A significant percentage of the absorber site environment does not contribute significantly to the total signal. In particular, the coordination number $N_j$ may be smaller than in the real configuration.

In a qualitative approach, the observation of the Fourier transform spectra obtained for different amorphous alloy compositions provides useful information on the local atomic environment which must be consistent for all concentrations and both edges. Figures 1(a) and 1(b) present the Fourier transform spectra obtained for the four compositions at the Ti K edge and Ni K edge respectively. At both edges a broad, weak first peak is observed, together with the absence of secondary peaks which would be characteristic of crystalline order. In amorphous alloys, only first neighbour atoms generally contribute to the EXAFS signal.

When the Ti atom content increases, the following observations can be made: (1) a simultaneous decrease in the peak magnitude for both Ti and Ni K edges; (2) a weak variation in the main peak position at the Ni K edge (except for $x=0.30$); (4) a progressive shift of the main peak in the large distance range at the Ti K edge.

Our first thought was to associate the magnitude of the local structural disorder with the titanium concentration in the alloy, *i.e.* the local disorder seems to be increased when the Ti atom content increases. In order to explain these experimental facts, we tested the following model of the local environment: a set of Ni–Ni bonds centred around a distance close to that found in pure crystalline nickel (represented by the parameter couple ($N_{NiNi}$, $R_{NiNi}$)); a set of Ti–Ti bonds centred around a distance close to that found in either pure titanium or crystalline TiNi compounds ($N_{TiTi}$, $R_{TiTi}$);

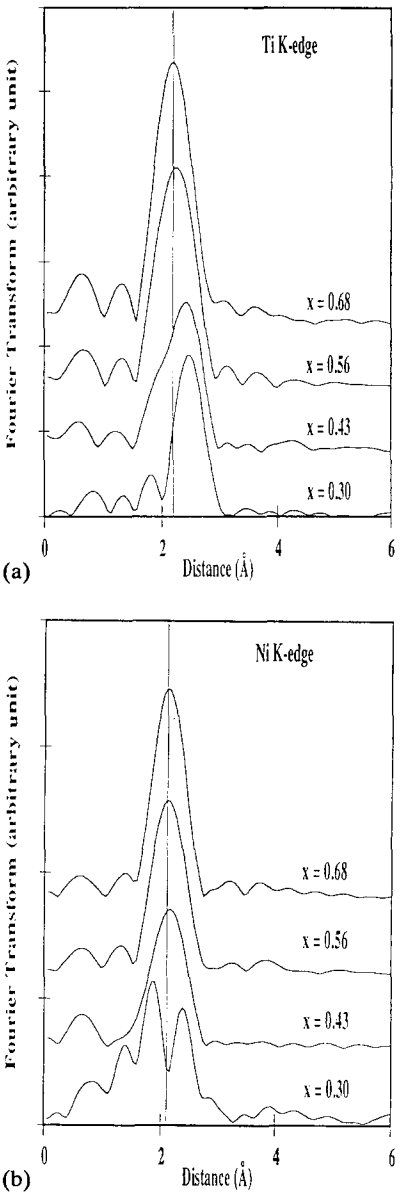


Fig. 1. Fourier transforms at the Ti K edge (a) and Ni K edge (b) for different $Ni_xTi_{1-x}$ amorphous alloy compositions ($x=0.68$, 0.56, 0.43 and 0.30 at.%).

a set of unlike Ti–Ni bonds centred around a distance intermediate between the two previous values. The distribution may vary when increasing the Ti atom concentration in order to take into account the asymmetric shape of the main peak in the large distance range. The topological disorder may be taken into account either by increasing the MSRD factor or by including several atomic subshells with different distances and partial coordination numbers. The first approach, involving a large increase in the MSRD factor and a single shell, has been rejected since it appears to limit drastically the simulation method. The second approach, involving several subshells assumed to have identical MSRD factors, leads to good fits, although

it introduces more floating parameters. This model has already been used theoretically [12] and experimentally [23]. Before applying this environment model, some physical constraints must be fulfilled in the signal simulation. Their application states the maximum number of floating parameters to be used.

### 3.2. Calculation constraints for amorphous signal simulation

According to the Shannon theorem [24], the number of independent parameters $N_{ind}$ is given by $N_{ind} = 2\delta k \delta R/\pi$, where $\delta R$ is the width of the main peak of the Fourier transform and $\delta k$ is defined by the energy range of the Hamming window. In our case we obtain $N_{ind} = 7$ for each spectrum. Since we use a least-squares fitting procedure, the number of floating parameters is limited to $N_{ind} - 1 = 6$ for one spectrum. Fortunately, we measured the EXAFS spectra at both edges (Ti and Ni) and in each case the interatomic distribution of unlike species must be conserved. In particular, the following constraining relations must hold

$$C_A N_{AB,i} = C_B N_{BA,i} \quad (3)$$

$$R_{AB,i} = R_{BA,i} \quad (4)$$

$$\sigma_{AB,i} = \sigma_{BA,i} \quad (5)$$

where $C_A$ ($C_B$) represents the concentration of the A (B) element in the material, $N_{AB,i}$ ($N_{BA,i}$) is the number of B atoms (A atoms) surrounding an A atom (B atom) in the subshell $i$ and $R_{AB,i}$ ($R_{BA,i}$) is the distance separating the central absorber A atom (B atom) from the B atom (A atom) in subshell $i$. Relation (3) takes into account the fact that the same total number of unlike atom pairs A–B must hold at both edges. Relations (4) and (5) allow an identical interatomic distance as well as an identical MSRD factor for each studied K edge. The total number of unlike atom pairs $N_{AB}$ will be defined by: $N_{AB} = \Sigma_i N_{AB,i}$.

Moreover, another constraint is to verify that EXAFS results agree with electron diffraction data found for the same concentration [9]. In particular, the interatomic distances obtained from the electron diffraction pattern ($R_{Diffraction}$) must be of the same order of magnitude as the average interatomic distances extracted from EXAFS data

$$R_{EXAFS} \approx R_{Diffraction} \quad (6)$$

with $R_{EXAFS} = C_A R_A + C_B R_B$
and $R_A = [\Sigma_i (N_{AB,i} R_{AB,i}) + N_{AA} R_{AA}]/N_A$

Our fitting procedure involves the use of both edge spectra simultaneously. The number of possible floating parameters ($2N_{ind} - 1$) becomes 12 when working with two edges. Shifts in the threshold energy ($\Delta E_0$(Ni) and $\Delta E_0$(Ti)) vary independently for both edges, but only one MSRD parameter ($\sigma$) is used. Therefore nine variable parameters are allowed to describe the titanium and nickel local atomic environments. Four are related to the like atom pairs ($N_{NiNi}$, $R_{NiNi}$, $N_{TiTi}$ and $R_{TiTi}$) so that five variable parameters remain for the unlike atom pair distribution. In order to reduce the number of floating parameters, we first fit the spectra with two separate subshells of Ni–Ti pairs. These variable parameters are denoted by ($N_{TiNi,1}$, $R_{TiNi,1}$) and ($N_{TiNi,2}$, $R_{TiNi,2}$) at the Ti K edge. The corresponding values at the Ni K edge are obtained using eqns. (3) and (4).

We do not use relation (6) to modify the number of floating parameters, but to give an additional physically meaningful indication to our results.

### 3.3. Calculation details and fitting model for $Ni_{68}Ti_{32}$ alloy

For each edge, the aim of this work is to obtain the absorber environment as a function of the amorphous alloy composition. In order to provide an illustration of the application of the model we present, as an example, the different calculation steps used for the $Ni_{68}Ti_{32}$ alloy.

#### 3.3.1. Ti K edge

The Ti K edge EXAFS signal given in Fig. 2(a) shows more significant changes with alloy composition than those related to the Ni K edge (Fig. 2(b)). The experimental results were fitted using partial coordination numbers and interatomic distances as floating parameters for all three separate subshells (Ti–Ti, Ti–Ni, 1 and Ti–Ni, 2). As indicated above, the fit quality factor is based on the nodal positions. We obtained a number of solutions which are given in Fig. 3 as a function of the unlike atom ratio on two subshells ($x$ axis) and the total number of unlike atoms ($y$ axis). Each set of solutions corresponds to a different global number $N_{Ti}$. The interatomic distances do not change significantly and are always centred around $R_{TiNi,1} = 0.250 \pm 0.002$ nm and $R_{TiNi,2} = 0.279 \pm 0.002$ nm, the like atom pair being centred around $R_{TiTi} = 0.305 \pm 0.003$ nm. Solutions reported in Fig. 3 were obtained when the variance parameter (eqn. (2)) was less than twice its minimum value ($V_m = 0.1$ eV$^2$). We obtain good amplitude agreement over the whole energy range for $\sigma = 0.012 \pm 0.0005$ nm and $\Delta E_0 = 10$ eV. Such criteria provide an uncertainty of about 5% in the number of unlike atoms $N_{TiNi}$. The $N_{TiNi}/N_{Ti}$ ratio, which estimates the degree by which a titanium atom is surrounded by unlike nickel atoms, appears to be independent of the global atom number $N_{Ti}$ as shown in Fig. 3. This particular value is essential to fit the spectra and is related, as shown below, to the chemical order.

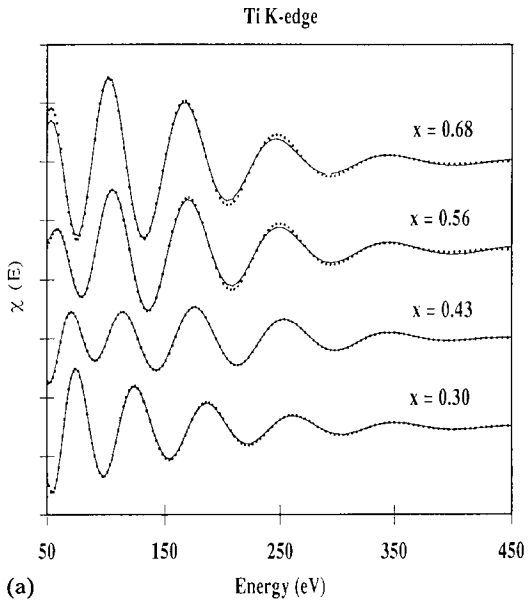


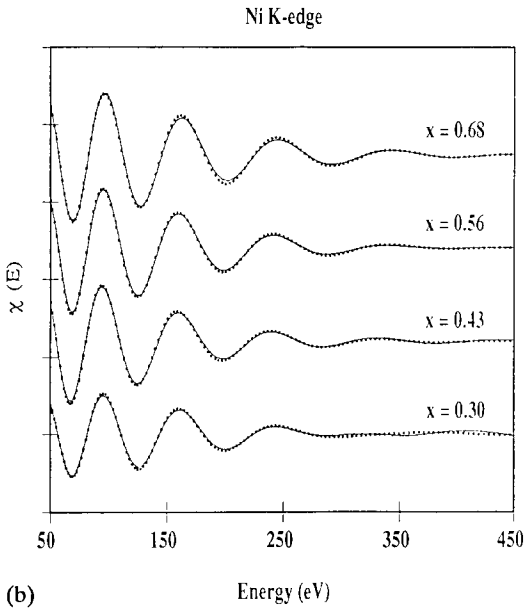


Fig. 2. Filtered backtransformed EXAFS spectra $\chi(E)$ at the Ti K edge (a) and Ni K edge (b) for different $Ni_xTi_{1-x}$ amorphous alloy compositions ($x=0.68$, 0.56, 0.43 and 0.30 at.%): —, simulation; · · · · ·, experimental.

### 3.3.2. *Ni K edge*

In a second step, we searched for a solution which is consistent at both edges, the structural parameters found at the Ti K edge being used at the Ni K edge. This solution must fulfil eqns. (3), (4) and (5) defined above. This step removes some solutions found at the Ti K edge and so allows us to determine the Ni–Ni distance and absolute atom pair number. The best solutions lead to $R_{NiNi}=0.245\pm0.002$ nm as in pure nickel with $\Delta E_0=5$ eV. This model provides a quasi-unique solution with respect to the defined error.

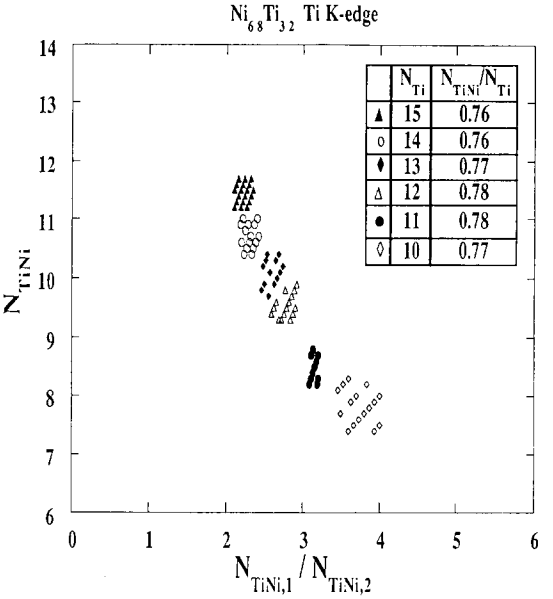


Fig. 3. $N_{TiNi}$ *vs.* $N_{TiNi,1}/N_{TiNi,2}$ ratio for the best solutions obtained in the case of $Ni_{68}Ti_{32}$ amorphous alloy at the Ti K edge.

TABLE 2. Structural parameters of $Ni_{68}Ti_{32}$ amorphous alloy extracted for EXAFS spectra simulations

| Central atom | $N_{AB}$ | Surrounder | $R_{AB}$ (nm) | $\sigma$ (nm) | $E_0$ (eV) |
|---|---|---|---|---|---|
| Ni | 6 | Ni | 0.245 | 0.012 | 5 |
| | 3.25 | Ti | 0.251 | 0.012 | 5 |
| | 1.25 | Ti | 0.279 | 0.012 | 5 |
| Ti | 7.25 | Ni | 0.251 | 0.012 | 10 |
| | 2.75 | Ni | 0.279 | 0.012 | 10 |
| | 2.5 | Ti | 0.305 | 0.012 | 10 |

When the MSRD factor is chosen to be the same for each subshell, it is expected to lead to erroneous results, particularly for alloys which have a tendency for unlike atom pair formation, as a larger MSRD value is expected for the like atom pair. This may induce a larger number of like atom pairs (Ni–Ni or Ti–Ti) in the atomic distribution in order to compensate for the disorder effect on the amplitude. However, if we increase the MSRD value, the fit (the amplitude and even the phase) in the low energy range rapidly becomes unreliable. For all acceptable fits performed, the results do not shift significantly from those related to the quoted structural parameters. A complete description of the structural parameters is given in Table 2.

### 3.4. *CSRO parameter and results*

In amorphous compounds, the strong signal damping with increasing energy means that important topological disorder exists which varies around each atomic site even for the same species. The mean disorder magnitude is taken into account by the MSRD factor which is

chosen to be identical for each subshell. The CSRO calculated using the partial coordination numbers therefore depends on the above assumption. The CSRO parameter can be deduced from the environment of each absorber atom as follows

$$\alpha_{AB} = 1 - N_{AB}/NC_B$$

and

$$\alpha_{BA} = 1 - N_{BA}/NC_A$$

where $N = C_A N_A + C_B N_B$ is the average coordination number in the compound and $N_A = N_{AA} + N_{AB}$ ($N_B = N_{BB} + N_{BA}$) is the number of atoms surrounding an A atom (B atom). In these conditions we must obtain

$$\alpha_{AB} = \alpha_{BA} = \alpha \quad (7)$$

This coefficient, also called the Cowley–Warren parameter [25], gives the statistical distribution with respect to unity. It is calculated with the average coordination number $N$ which yields a global value of the chemical order. For a random distribution $\alpha$ vanishes, whereas it becomes negative for systems with preferred unlike atoms as nearest neighbours. The $\alpha$ value depends on the definition adopted for $N_{AB}$ and comparison with other published results is only possible when $N_{AB}$ values and the CSRO parameter have been determined in the same manner. For example, for electron diffraction, the coordination number depends on the maximum value chosen for the interatomic distance in the first shell.

For the four amorphous compositions studied, the Ni–Ni and Ni–Ti pairs are centred around the following interatomic distances with a maximum fluctuation of about 0.003 nm from one concentration to another: $R_{NiNi} = 0.247$ nm; $R_{TiNi,1} = 0.250$ nm; $R_{TiNi,2} = 0.278$ nm. Simultaneously, the Ti–Ti interatomic distances decrease with titanium content from 0.305 nm to 0.286 nm.

It should be noted that a slightly more complex model can be used which gives more satisfactory results with increasing titanium content. This model involves the splitting of the NiTi, 2 subshell into two subshells having the same partial coordination number and centred around $R_{TiNi,2} = 0.278$ nm. This introduces only one additional floating distance parameter and the Shannon theorem condition is still fulfilled.

The main results are given in Table 3 which includes the partial coordination number of atoms surrounding Ti and Ni species, the average coordination number $N$ and the CSRO order parameter obtained from these calculations. The average interatomic distances extracted from EXAFS data are compared with those deduced from electron diffraction ring positions [9]. The uncertainty in the $N_{Ti}$ and $N_{Ni}$ values is about 5% and thus the CSRO parameter values are given with an error of $\Delta\alpha = \pm 0.03$. The average interatomic distances are determined with an uncertainty of about $\pm 0.005$ nm. For all the compositions, and at both edges, the MSRD values have been found to be $\sigma = 0.012 \pm 0.0005$ nm.

TABLE 3. Coordination numbers, CSRO parameters and average interatomic distances measured for different $Ni_xTi_{1-x}$ amorphous alloy compositions

| | Parameter | $x$ (at.%) | | | |
|---|---|---|---|---|---|
| | | 0.68 | 0.56 | 0.43 | 0.30 |
| Ti K edge | $N_{TiTi}$ | 2.5 | 3.5 | 4.25 | 6 |
| | $N_{TiNi}$ | 10 | 8.5 | 6.25 | 4.5 |
| | $N_{Ti}$ | 12.5 | 12 | 10.5 | 10.5 |
| Ni K edge | $N_{NiNi}$ | 6 | 5 | 3.75 | 2.5 |
| | $N_{NiTi}$ | 4.5 | 6.5 | 8.25 | 10.5 |
| | $N_{Ni}$ | 10.5 | 11.5 | 12 | 13 |
| | $N$ | 11 | 11.5 | 11 | 11.5 |
| | $\alpha$ | −0.29 | −0.28 | −0.30 | −0.33 |
| | $R_{EXAFS}$ (nm) | 0.256 | 0.261 | 0.265 | 0.273 |
| | $R_{Diffraction}$ (nm) | 0.257 | 0.260 | 0.265 | 0.275 |

## 4. Discussion

### 4.1. Structural parameters

With increasing titanium concentration, $N_{Ti}$ decreases and $N_{Ni}$ increases. This can be related to the chemical ordering of these alloys: around one atom type, unlike atom pair formation is favoured. A more well-organized environment is expected around the less concentrated atom in the alloy, especially when considering the same topological disorder (MSRD) for all subshells.

The average coordination numbers remain almost constant (11–11.5) for all the alloys studied. This value is smaller than the global coordination number which is found to be 15 by electron diffraction [9] on the same samples. It should be noted that these authors have calculated $N$ through the integral $N = \int_0^{R_{min}} R(r)dr$ where $R_{min} = 0.360$ nm is the position of the first minimum after the first peak of the experimental radial distribution function $R(r)$. Moreover, as previously discussed the coordination number obtained from EXAFS data may be damped in amorphous material.

A comparison between EXAFS and electron diffraction results [9] shows excellent agreement for the average interatomic distances. In addition, in both cases the average distance increases with the Ti atom content, the values being lower than those predicted by Vegard's law. This again indicates the existence of CSRO which favours short Ti–Ni bonds rather than long Ti–Ti bonds. This result may be understood in terms of the difference

between the atomic radii since Ni atoms are smaller than Ti atoms.

Another factor is also related to the existence of CSRO. It was mentioned above that the distances separating two titanium atoms decrease with increasing titanium content. In other words, when the Ti concentration is low, more Ti–Ni bonds exist due to the chemical ordering tendency and thus the Ti–Ti bonds are forced to be larger.

The MSRD value ($\sigma_{amorph} = 0.012 \pm 0.0005$ nm) used in this work to fit all the amorphous alloy spectra accurately is larger than that of the reference crystalline material used to determine the backscattering amplitudes and phases ($\sigma_{cryst} = 0.009 \pm 0.001$ nm). In both cases, a gaussian distribution is used. However, the description of a large disorder involves an asymmetrical distribution of distances peaked at $R_p$ rather than a perfectly symmetrical distribution. The use of a more complex function introduces, in the EXAFS formula, additional terms which modify the phase and amplitude signal variations *vs.* energy. Firstly, the second-order cumulant $C_2$ takes into account the width and asymmetrical degree of the distance distribution. Starting from an apparent value $C_2 = 0.012$ nm$^2$, we have built a distribution set which yields the same amplitude behaviour by adding two different gaussian functions: the first part is related to $r < R_p$ and is built with $\sigma^- < 0.012$ nm and the second part is related to $r > R_p$ with $\sigma^+ > 0.012$ nm. The more asymmetrical case must be limited to $\sigma^- = 0.009$ nm, which represents the basis MSRD factor related to the experimental reference signal. We considered this extreme case in order to calculate the maximum errors obtained when using a gaussian distribution. The $k$ term deals with a shift of the interatomic distances without modifying the variance calculation. The additional term $k^3$ introduces a non-linear phase shift which can be approximated, in the energy range used, by a linear law with a correlation factor of 0.985. Such an approximation gives a variance error of about 0.07 eV$^2$ which is still below those given by the signal fits obtained previously (0.1 eV$^2 < V <$ 0.2 eV$^2$). Thus, when using an asymmetrical distribution, calculations provide results consistent with those deduced from the EXAFS formula (eqn. (1)), but with a distance shift of about $\delta R = 0.006$ nm. The coordination numbers are unaffected if the same asymmetrical distribution is used for each subshell.

The EXAFS signal amplitude may be affected by the additional term $k^4$ ($\exp(2/3C_4k^4)$, $C_4$ is the fourth-order cumulant) which starts to modify the spectral amplitude significantly (greater than 10%) for $k$ values up to 100 nm$^{-1}$. As the fitting is performed between 40 and 120 nm$^{-1}$, we consider that the use of a gaussian distribution only slightly affects the coordination numbers deduced. The $k_4$ term is positive and its application would provide a smaller MSRD value. Moreover, the distance shift mentioned above is too important (with regard to the electron diffraction results). Therefore, our asymmetrical approach is too drastic and the real effect is less pronounced. Indeed, the variance error mentioned above is too large. Thus it can be concluded that the distortions obtained using the asymmetrical model do not considerably affect the pair distribution given in Table 3.

### 4.2. *Application of Miedema's model to EXAFS results*

It has been shown by Miedema and Dechatel [13] that the CSRO may be related to the crystallization enthalpy of amorphous alloys. According to this semi-empirical model, the crystallization enthalpy of an amorphous alloy may be written as

$$\Delta H_{cryst} = C_A \, \Delta H_B^{A,sol} (F_B^{A}{}_{cryst} - F_B^{A}{}_{amorph})$$

where $\Delta H_B^{A,sol}$ is the solid solution enthalpy of atoms A in the matrix consisting of B atoms. A labels the smallest atom (Ni in our case), $C_A$ is the fraction of A atoms and $F_B^A$ represents the degree by which an A atom is surrounded by B neighbours. $F_B^A$ is written as

$$F_B^A = N_{AB} S_B / (N_{AA} S_A + N_{AB} S_B)$$

where $S_A$ and $S_B$ are the surface sections of atoms A and B respectively. In this model, and depending on the CSRO in the alloy, the $F_B^A$ parameter can take all values between a minimum $C_B^s$, corresponding to the random atomic distribution, and a maximum $C_B^s[1 + 8(C_B^s C_A^s)^2]$, corresponding to complete chemical order [14].

From our EXAFS results, it is possible to extract an $F_{Ti}^{Ni}$ value which defines experimentally the degree by which an Ni atom is surrounded by Ti neighbours. In our case, $F_{Ti}^{Ni}$ is given by

$$F_{Ti}^{Ni} = N_{Ti} R_{Ti}^2 / (N_{Ni} R_{Ni}^2 + N_{Ti} R_{Ti}^2)$$
$$= (1 + 0.71 N_{Ni}/N_{Ti})^{-1}$$

with $R_{Ni} = 0.138$ nm and $R_{Ti} = 0.162$ nm [26]. For a random disordered solution we obtain

$$F_{Ti}^{Ni} = C_{Ti}^s = (1 + 0.71 C_{Ni}/C_{Ti})^{-1}$$

where $C_{Ti}^s$ represents the surface concentration of titanium atoms around an Ni central atom. For a fully ordered alloy and according to Miedema's model, $F_{Ti}^{Ni}$ is defined by

$$F_{Ti}^{Ni} = C_{Ti}^s [1 + 8(C_{Ti}^s C_{Ni}^s)^2]$$

The variations in $C_A^s F_B^A$ *vs.* $C_A^s$ have been plotted previously by Weeber [14]. The $F_B^A$ values were obtained from experimental measurements of crystallization enthalpies for several alloys, *e.g.* NiZr [27], FeZr, CuZr, CoZr [28] and NiTi [29]. We have also represented

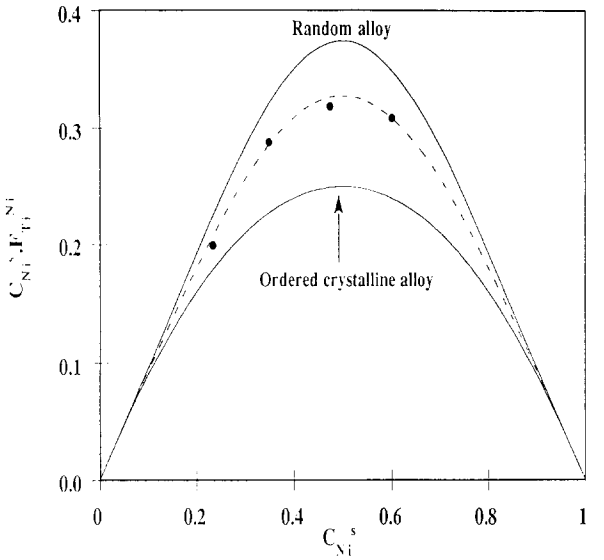


Fig. 4. $C_{Ni}{}^s F_{Ti}{}^{Ni}$ *vs.* $C_{Ni}{}^s$ for $Ni_xTi_{1-x}$ amorphous compounds (●). The upper curve represents the ordered crystalline alloy with $F_{Ti}{}^{Ni} = C_{Ti}{}^s[1 + 8(C_{Ni}{}^s C_{Ti}{}^s)^2]$ and the lower curve represents the random alloy with $F_{Ti}{}^{Ni} = C_{Ti}{}^s$. The broken line represents $F_{Ti}{}^{Ni} = C_{Ti}{}^s[1 + 5(C_{Ni}{}^s C_{Ti}{}^s)^2]$.

the variations in $C_{Ni}{}^s F_{Ti}{}^{Ni}$ deduced from EXAFS structural parameters *vs.* $C_{Ni}{}^s$ (Fig. 4). These values are compared with the limit values corresponding to a random alloy ($F_{Ti}{}^{Ni} = C_{Ti}{}^s$) and to an ordered alloy ($F_{Ti}{}^{Ni} = C_{Ti}{}^s[1 + 8(C_{Ti}{}^s C_{Ni}{}^s)^2]$). As shown in Fig. 4 our experimental values for the four concentrations studied are located between these two curves and approximately verify that $F_{Ti}{}^{Ni} = C_{Ti}{}^s[1 + 5(C_{Ti}{}^s C_{Ni}{}^s)^2]$. Our results are similar to those obtained by Weeber [14] on several other amorphous alloys.

## 5. Conclusions

We have performed an EXAFS analysis of amorphous $Ni_xTi_{1-x}$ alloys. A model has been proposed which enables us to determine the local environment consistent for both Ti and Ni K edge signals. For the four concentrations studied, the best fit of the EXAFS function is found for one shell of like atom pairs (Ni–Ni or Ti–Ti) and several subshells of unlike atom pairs (Ni–Ti or Ti–Ni) which are equivalent to an asymmetrical distribution. From these structural parameters, we have obtained the Cowley–Warren parameter which is always negative indicating a tendency towards chemical order. From Miedema's semi-empirical model, we have found chemical short range order which is intermediate between that found in a random alloy and an ordered crystalline alloy.

## References


1 D. E. Polck, A. Calka and B. C. Giessen, *Acta Metall., 26* (1978) 1097.
2 H. Ruppersberg, D. Lee and C. N. J. Wagner, *J. Phys. F, 10* (1980) 1645.
3 M. Sakata, N. Cowlan and A. A. Davies, *J. Non-Cryst. Solids, 61* (1984) 343.
4 C. N. J. Wagner and D. Lee, *J. Phys. (Paris), Colloq., 41* (8) (1980) 242.
5 K. H. J. Buschow, *J. Phys. F, 13* (1983) 563.
6 P. Moine, A. Naudon, J. J. Kim, A. F. Marshall and D. A. Stevenson, *J. Phys. (Paris), Colloq.,* (1985) 223.
7 K. Zöltzer and R. Bormann, *J. Less-Common Met., 140* (1988) 335.
8 J. J. Kim, P. Moine and D. A. Stevenson, *Scr. Metall., 20* (1986) 243–248.
9 P. Moine, J. Delage, A. R. Pelton and R. Sinclair, *Acta Metall. Mater., 40* (1992) 1855.
10 L. Battezzati, S. Enzo, L. Schiffini and G. Cocco, *J. Less-Common Met., 145* (1988) 301.
11 S. Enzo, L. Schiffini, L. Battezzati and G. Cocco, *J. Less-Common Met., 140* (1988) 129.
12 D. Gazzillo, G. Pastore and S. Enzo, *J. Phys. Condensed Matter, 1* (1989) 3469–3487.
13 A. R. Miedema and P. F. Dechatel, in L. H. Bennet (ed.), *Theory of Alloy Phase Formation,* 1979, p. 334.
14 A. Weeber, *J. Phys. F, 17* (1987) 809.
15 P. Moine, A. Naudon, J. J. Kim, A. F. Marshall and D. A. Stevenson, *J. Phys. (Paris), Colloq., 46* (1985) 223.
16 P. A. Lee and J. B. Pendry, *Phys. Rev. B, 11* (1975) 2795.
17 P. A. Lee and G. Beni, *Phys. Rev. B, 15* (1977) 2862.
18 E. A. Stern, B. A. Bunker and S. M. Heald, *Phys. Rev. B, 21* (12) (1980) 5521.
19 F. Laves and H. J. Wallbaum, Die Kristallstruktur von $Ni_3Ti$ und $Si_2Ti$, *Z. Krist., A101* (1939) 78.
20 A. G. McKale, G. S. Knapp and S. K. Chan, *Phys. Rev. B, 33* (1986) 841.
21 A. Yurko, J. W. Barton and J. G. Parr, *Acta Crystallogr., 12* (1959) 909.
22 G. Bunker, *Nucl. Instrum. Methods, 207* (1983) 437.
23 A. Sadoc, D. Raoux, P. Lagarde and A. Fontaine, *J. Non-Cryst. Solids, 50* (1982) 331–349.
24 J. Max, in Masson (ed.), *Méthodes et Techniques de Traitement du Signal,* Paris, 1971, p. 64.
25 B. E. Warren, *X-Ray Diffraction,* Addison–Wesley, MA, 1969, p. 227.
26 W. H. McMaster, N. K. Delgrande, J. H. Mallet and J. H. Hubbel, *Lawrence Livermore Laboratory, Report, Sec 2, Rev I,* 1969.
27 M. P. Henaff, C. Colinet, A. Pasturel and K. H. J. Buschow, *J. Appl. Phys., 56* (1984) 307.
28 Z. Altounian, R. J. Shank and J. O. Strom-Olsen, *J. Appl. Phys., 58* (1985) 1192.
29 K. H. J. Bushow, *Solid State Commun., 43* (1982) 171.